Modelling the operation of vehicles at signalised intersections with special width approach lane based on field data

Zhao, Jing; Kiptoo Kigen, Kevin ; Wang, Meng

DOI
10.1049/iet-its.2020.0157

Publication date
2020

Document Version
Accepted author manuscript

Published in
IET Intelligent Transport Systems

Modelling the operation of vehicles at signalized intersections with special width approach lane based on field data

Jing Zhao [1,2*], Kevin Kiptoo Kigen [1], Meng Wang [2]

[1] Department of Traffic Engineering, University of Shanghai for Science and Technology, Shanghai, China
[2] Transport & Planning, Delft University of Technology, Delft, Netherlands
[*]jing_zhao_traffic@163.com

Abstract: The intersection with special width approach lane (SWAL) is a newly proposed unconventional intersection design. A microscopic traffic flow model was proposed for describing the operation of vehicles at signalized intersections with SWAL. The operation process of driving on the SWAL was divided into four segments, including entering segment, transition segment, special width lane segment, and exiting segment. The car-following and lane selection behaviours of vehicles in these segments are analysed. The parameters used in the model were calibrated using the field data collected in Germany. The proposed model was realized in a time-discretized simulation. The sensitivity analysis of geometric, traffic, and signal factors were conducted. The results show that for the car-following behaviour, the passenger cars on the narrowed lanes cannot drive as efficient as on the normal width lane. For lane selection behaviour, it mainly depends on the distance between the two nearest vehicles in front on the two narrow lanes. The effectiveness of the SWAL depends on whether it is long enough to accommodate the queuing vehicles, which is a combined result of the layout design and the signal timing.

1. Introduction

To date, there has been an influx in the number of vehicles in many cities all over the world. The main reason for this is the economic growth and development that has necessitated car ownership as a need rather than a luxury. The increase in traffic demand has deteriorated bottleneck problems on the road infrastructure, especially during the rush hours.

To alleviate traffic problems, researchers and engineers have designed different solutions to traffic problems. Substantial attention devoted to the congested urban intersections, because more and more signalized intersections are operated with oversaturated conditions. This has led to the proposals of diverse designs that are unconventional to improve the capacity of intersections, such as median U-turn intersections [1, 2], superstreet intersections [3, 4], uninterrupted flow intersections [5], displaced left-turn intersections [6, 7], exit-lanes for left-turn intersections [8-10], tandem intersections [11-14], and special width approach lane intersections (SWAL) [15].

Of particular interest to this study is the intersection with special width approach lane (SWAL). The idea of narrowing carriageway for providing space for cyclists on urban streets [16, 17] and for providing more traffic lanes on unban freeways [18] was proposed in previous studies. Moreover, the concept of the shared space was promoted [19], and the interactions between the vehicular flow, cyclist flow, and pedestrian flow were studied in recent years [20-22]. Inspired by these studies, the SWAL was proposed [15].

The SWAL consists of two narrow lanes that are utilized by either two passenger cars or one heavy vehicle. Under traditional designs, the lane width should be sufficient to accommodate the width of the design vehicles. Since the width of the buses and trucks are usually 2.4-2.6 m, a lane less than 3.0 m wide may be hard for them to progress. Therefore, a lane width of 3.3 m is used quite extensively for urban arterial street designs [23]. The design of the SWAL aims to increase the number of approach lanes while retaining the operational safety of heavy vehicles by offering lane width flexibility. The SWAL can be used by two passenger cars on two narrow lanes, while heavy vehicles use it as one lane. This is the main difference between the SWAL and traditional designs.

In the existing studies on such design, the ideal state of the regular operations of the vehicles is assumed. However, the reduced lane width may pose a challenge to some drivers. It may lead to behavioural adaptation in terms of the decisions and perception-reaction of the drivers [24, 25]. Individual traits such as conservative, neutral, and aggressive profiles of drivers will have varying impacts on lane selection and saturation flow. Moreover, willingness to travel side by side (lateral positions) will also impact on the car-following behaviour of vehicles on the special width lane. These potential changes in operation are not taken into much consideration in the existing layout and signal control optimization models.

In the research field of traffic flow, various microscopic models have been established to describe the operation of vehicles and analyse different complex traffic phenomena at both highways and urban roads [26-28].

The car-following model is one of the most important parts in the field of microscopic traffic flow, which describes the running status of the vehicle under the influence of the surrounding vehicles. It can be divided into the stimulus-response model, collision avoidance model, driving psychophysical model, and artificial intelligence-based model [29]. Among them, the optimal velocity model has received extensive attention due to its analytical tractability and ease to simulate. A series of improved models under

different conditions have been proposed. The typical research results include generalized force model [30], optimal velocity (OV) model [31], full velocity difference (FVD) model [32], and full velocity and acceleration difference (FVAD) model [33]. Some other studies focus on modelling the two-dimensional movement at intersections [34]. Previous microscopic traffic flow models emphasized in numerous influencing factors [35-38]. From these studies, the microscopic traffic flow models have been used to simulate single and multiple vehicle-driver units and describe traffic flow in signalized intersections.

Although the existing models can describe the microcosmic properties of the traffic flow, they do not explicitly reproduce the impact of the special traffic lane design (SWAL) on the driving behaviour and the corresponding changes in traffic flow. It is because the lane selection of the two narrow lanes should be considered for passenger cars. Moreover, the heavy vehicles should occupy the two narrow lanes, which will affect both the car-following behaviour.

This study aims to extend the microscopic traffic flow model for driving on the SWAL based on field data to reflect the operational characteristics of the intersections with SWAL. The car-following and lane selection behaviours of vehicles on the SWAL are analysed. The rest of the paper is arranged as follows. The data collection is conducted in section 2. The model is established in section 3. The proposed model is calibrated and validated in section 4. The simulation realization is introduced in section 5. The sensitivity of key parameters is analysed in section 6. The conclusions are drawn in section 7.

2. Data collection

As shown in Fig. 1, the geometric design characteristic of SWAL lies in that it is consists of two narrow approach lanes (about 2.6 m wide for each narrow lane). Under such a design, two passenger cars are possible to travel alongside each other. For heavy vehicles, they use the SWAL as a single lane and occupy the two narrow approach lanes. Under traditional designs, the lane width should be sufficient to accommodate the width of the design vehicles. The lanes are operated independently, and the vehicles do not occupy two traffic lanes (except for the lane changing). The difference in the geometric design and traffic rules between the SWAL and traditional designs causes the difference in operation.

The SWAL design has been applied in Karlsruhe, a southwestern city in Germany. The four intersections with SWAL design were selected for data collection. They are Rheinstrasse - Philippstrasse, Rheinstrasse - Nuitsstrasse, Rheinstrasse - Am Entenfang, Karlstrasse - Amalienstrasse, as shown in Fig. 2.

The data were collected by a video camera, which was mounted at the side of the street. The collection of data was carried out for 6 hours at each intersection. The video recordings were collected during morning peak hours of 7 am to 9 am and the evening peak hours between 4 pm and 6 pm to ensure sufficient data collection and also to ensure proper visibility.

A video data processing software, which has been successfully used in the development of the Highway Capacity Manual of Shanghai, is used in the extraction of the data [39, 40]. Then, the position of each vehicle at each discrete 0.1 seconds can be obtained. Then, the speed and acceleration can be obtained accordingly. From the video, one can find that most of the passenger cars observed would tend to use single lane in special width lane section, while heavy vehicles occupy both lanes, as shown in Fig. 3.

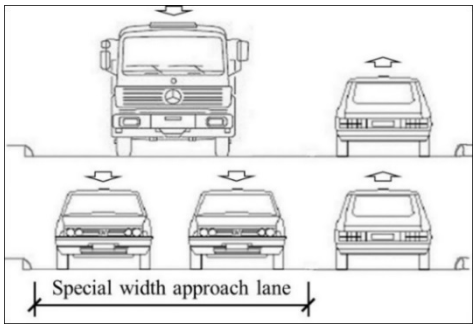

Fig. 1. *Design idea of SWAL*[15]

(a) Rheinstrasse - Philippstrasse intersection

(b) Rheinstrasse - Nuitsstrasse intersection

(c) Rheinstrasse - Am Entenfang intersection

(d) Karlstrasse - Amalienstrasse intersection

Fig. 2. *Surveyed intersections*

(a) Passenger cars use single lane in SWAL

(b) Heavy vehicles occupy both lanes in SWAL

Fig. 3. *Operation in the real world*

3. Modelling

An approach with a special width lane is considered as the research object, as illustrated in Fig. 4. It contains four segments: (1) entering segment (normal lane segment), (2) transition segment, (3) special width lane segment, and (4) exiting segment. Due to the different geometric conditions of the different segments, the driving behaviour will vary. In this section, the car-following model will be established. The parameters in the model will be calibrated in section 4.

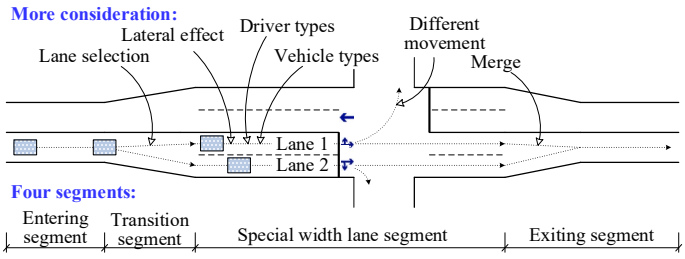

Fig. 4. *An approach with a special width lane*

3.1. Car-following model in the entering segment

In the entering section, since the width of the lane is normal, the traditional car-following models on a single lane can be used. According to the literature review, the optimal velocity model has received extensive attention among the existing car-following models. The full velocity difference (FVD) model is used in this study, as shown in Eq. (1).

$$\frac{\mathrm{d}v_n(t)}{\mathrm{d}t} = \kappa\left(V\left(\Delta x_n(t)\right) - v_n(t)\right) + \lambda \Delta v_n(t) \tag{1}$$

where $v_n(t)$ is the velocity of the vehicle n at time t, m/s; $\Delta x_n(t) = x_{n-1}(t) - x_n(t)$ is the space headway between vehicle n and vehicle n-1 at time t, m; $v_n(t)$ is the velocity of vehicle n at time t, m/s; $\Delta v_n(t) = v_{n-1}(t) - v_n(t)$ is the velocity difference between vehicle n and vehicle n-1 at time t, m/s; $V(.)$ is the optimal velocity function of the vehicle n, m/s, which can be selected as that proposed by Helbing and Tilch [30], as shown in Eq. (2); κ and λ are sensitivity parameters.

$$V\left(\Delta x_n(t)\right) = V_1 + V_2 \tanh\left(C_1\left(\Delta x_n(t) - l_c\right) - C_2\right) \tag{2}$$

where l_c is the length of the vehicle, m; V_1, V_2, C_1, C_2 are parameters.

3.2. Car-following model in the transition segment

In the transition segment, one normal traffic lane is divided into two narrow lanes. The drivers of passenger cars should decide which narrow lane to choose, which further affects which car to follow. The basic car-following model is the same as that of the segment 1. The difference lies in that a decision should be made which car to follow. Therefore, this section is mainly about lane change.

The outcome of the lane selection behaviour is binary: lane 1 or lane 2. Therefore, the logistic regression model is suitable for modelling the lane selection behaviour. The following two influencing factors are considered. The first one is the distance between the two nearest vehicles in front on different lanes, $\Delta x_n^{L12}(t)$, given by Eq. (3). The second one is the velocity difference between the two nearest vehicles in front on different lanes, $\Delta v_n^{L12}(t)$, given by Eq. (4). The reasons for selecting the two potential influencing factors are two-folder. First, car-following behaviour is mainly related to the space headway and the velocity difference between vehicles [32, 41]. Second, achieving higher speeds is one of the main purposes for lane changing of vehicles [42, 43].

$$X_1 = \Delta x_n^{L12}(t) = x_n^{L2}(t) - x_n^{L1}(t) \tag{3}$$

$$X_2 = \Delta v_n^{L12}(t) = v_n^{L2}(t) - v_n^{L1}(t) \tag{4}$$

where $x_n^{L1}(t)$ and $x_n^{L2}(t)$ are the position of the nearest vehicle in front on lanes 1 and 2 at time t; $v_n^{L1}(t)$ and $v_n^{L2}(t)$ are the velocity of the nearest vehicle in front on lanes 1 and 2 at time t.

Then, the utility of selecting lane 2, which is derived from the multiple linear regression function, can be specified as Eq. (5). It is the linear sum of β_0 plus the products of coefficients and their corresponding independent variables. Please note that the utility function for lane selection, as shown in Eq. (5), can be replaced by any suitable models without changing the framework of the proposed model. The protentional influencing factors, such as the characteristic of the driver (plan-ahead distance and aggressiveness) [44] and the layout of the lane assignment [14, 45], can be added in Eq. (5).

$$U = \beta_0 + \beta_1 X_1 + \beta_2 X_2, \tag{5}$$

where U is the utility of selecting lane 2; X_1 and X_2 are the influencing factors of the lane selection, namely $\Delta x_n^{L12}(t)$ and

$\Delta v_n^{L12}(t)$; β_0 is a constant term representing the intercept, which indicates the lane that the vehicles prefer when the condition is the same; and β_1 and β_2 are parameters associated with the influencing factors and quantifies their relationship with the outcome variable.

With the probability of selecting lane 2 and lane 1 denoted $p(U)$ and $p(1\text{-}U)$ respectively, then the probability of selecting lane 2 can be calculated using the Logit function, as shown in Eq. (6).

$$p(U)=\frac{1}{1+e^{-U}}, \tag{6}$$

where $-\infty < U < +\infty$, $0 < p(U) < 1$.

As U approaches -∞, p approaches 0, and as U approaches ∞, p approaches 1. In the model, any $p(U)$ value closer to 0 means that the probability for drivers to select lane 2 is very low (closer to 0%) while a value closer to 1 means that the event of selecting lane 2 is very likely to occur (closer to 100%). Then, the probability $p(U)$ can be compared with a threshold value R to determine the decision. If $p(U) \geq R$, lane 2 will be select, otherwise, lane 1 will be selected. Since there are only two narrow lanes to select, the $p(U)$ value larger than 0.5 means that the probability of selecting lane 2 is higher than that of lane 1. On the contrary, the $p(U)$ value smaller than 0.5 means that the probability of selecting lane 1 is higher than that of lane 2. We assume that drivers are utility maximisers and select the lane with higher probability (utility). Therefore, the threshold value R is set to 0.5.

Apart from the through passenger cars, there is no need for the other three types of vehicles, namely left-turn, right-turn and heavy vehicles, to make a lane selection. The left-turn and right-turn vehicles should select the left-most lane (lane 1) and right-most lane (lane 2), respectively. The heavy vehicles have to occupy both two lanes because the width of a narrow lane cannot accommodate it.

Therefore, lane selection can be given by Eq. (7). Motion behaviour is the same as Eq. (1).

$$L_n=\begin{cases}\lceil p(U)-R\rceil+1 & (H_n=0, M_n=2)\\ 1 & (H_n=0, M_n=1)\\ 2 & (H_n=0, M_n=3)\\ 3 & (H_n=1)\end{cases}, \tag{7}$$

where L_n is the selected lane for vehicle n, 1 for lane 1, 2 for lane 2, and 3 for the occupation of both two lanes; R is a threshold value between 0 and 1; H_n is a binary parameter indicating the type of the vehicle n, 1 for heavy vehicle and 0 for passenger car; M_n is a parameter indicating the turning movement of the vehicle n, 1 for left-turn, 2 for through movement, and 3 for right-turn.

3.3. Car-following model in the special width lane segment

In the special width lane section, passenger cars drive on one of the two narrows lanes, while heavy vehicles occupy two narrows lanes, which changes the car-following rules (which car to follow) and the parameters in the car-following model. Since the width of lanes is narrowed, the drivers should drive more cautiously to avoid the lateral scratches. Therefore, the optimal velocity will be affected. In the traditional FVD model, only the effect between the longitudinal vehicles is considered when calculating the optimal velocity. However, in the special width lane section, the effect from the lateral vehicles should be added because of the narrow lanes. The degree of the effect is related to the velocity of the vehicle in front on the adjacent lane, and the space headway between vehicle n and the vehicle in front on the adjacent lane. Therefore, the optimal velocity can be formulated as Eq. (8). Motion behaviour is the same as Eq. (1).

$$V(\Delta x_n(t))=V_1+V_2\tanh\left(C_1(\Delta x_n(t)-l_c)-C_2+C_3 v_n^A(t)+C_4\Delta x_n^A(t)\right) \tag{8}$$

where $v_n^A(t)$ is the velocity of the vehicle in front on the adjacent lane, m/s; $\Delta x_n^A(t)$ is the space headway between vehicle n and the vehicle in front on the adjacent lane, m; C_3 and C_4 are parameters.

3.4. Car-following model in the exiting segment

In the exiting segment, the through vehicles on the two narrow lanes have to merge into a lane. The following two principles are used to establish the car-following model: the vehicles on two narrow lanes have the same priority, and all vehicles should follow the principle of first come first service. Then, the vehicles will follow the vehicle in front in the exiting section when they touch the end of the special width lane section. Motion behaviour is the same as Eq. (1).

4. Model calibration and validation

In this section, 80% of the collected data is used to calibrate the proposed model, and the remaining 20% is used for the validation. Please note that different types of vehicles should have different parameters for the car-following model [46-48]. However, the traffic pattern at the surveyed site is uniform. During the survey period, the percentage of heavy vehicles is 1.0%. Therefore, we cannot calibrate the parameters for heavy vehicles.

4.1. Segment 1

A total of 1026 vehicles were observed from the selected zone with geometric properties that match an entering section. The nonlinear regression was conducted using the Levenberg-Marquardt estimation method. The method is typically suitable for fitting a parameterized function to a set of measured data points by minimizing the sum of squares of the errors between the data points and functions. The calibration results of the parameters in Eqs. (1) and (2) are shown in Table 1. The R-squared is 0.887.

Table 1 Parameter estimates of segment 1

Parameter	Estimate	Std. Error	95% Confidence Interval	
			Lower Bound	Upper Bound
κ	0.202	0.009	0.183	0.220
λ	0.442	0.008	0.426	0.457

V_1	6.477	0.302	5.884	7.070
V_2	11.244	0.589	10.087	12.400
C_1	0.130	0.009	0.111	0.148
C_2	1.645	0.137	1.376	1.914

The two-related-samples non-parametric test (Wilcoxon signed-rank method) was conducted to validate the accuracy of the model in segment 1. This method is carried out to compare two related samples to assess whether the population mean ranks differ. As shown in Table 2, there is no significant difference between the estimated results from the model and the measured values ($p > 0.05$). It indicates that the proposed model has acceptable goodness of fit and is effective to simulate the actual conditions of the phenomenon.

Table 2 Model validation of segment 1

Items	N	Mean Rank	Sum of Ranks
Negative Ranks	103[a]	108.90	11216.50
Positive Ranks	100[b]	94.90	9489.50
Ties	3[c]		
Total	206		
Z	-1.030		
Sig. (2-tailed)	0.303		

Note: a. Estimated < Measured; b. Estimated > Measured; c. Estimated = Measured

4.2. Segment 2

A sample size of 998 vehicles was observed during the data collection. The results of the logistic regression are shown in Table 3. It shows that the selection of the two narrow lanes is significantly related with the distance between the two nearest vehicles in front on different lanes ($p < 0.05$), but not significantly related with the velocity difference between the two nearest vehicles in front on different lanes ($p > 0.05$). Therefore, the velocity difference variable is omitted, and the logit model is re-calibrated. The regression results are shown in Table 4. We also analyse the relationship between the accuracy of the lane selection and the threshold value R. It is found that setting $R = 0.5$ can result in the highest accuracy in predicting the lane selection behaviour, as shown in Fig. 5.

Table 3 Original logistic regression

Items	B	S.E.	Wald	df	Sig.	Exp(B)
Constant	0.003	0.005	0.307	1	0.579	1.003
$\Delta x_n^{L12}(t)$	0.268	0.023	140.454	1	0.000	1.308
$\Delta v_n^{L12}(t)$	0.061	0.071	0.730	1	0.393	1.063

Table 4 Parameter estimates of segment 2

Items	B	S.E.	Wald	df	Sig.	Exp(B)
Constant	0.061	0.071	0.738	1	0.390	1.063
$\Delta x_n^{L12}(t)$	0.268	0.023	140.248	1	0.000	1.307

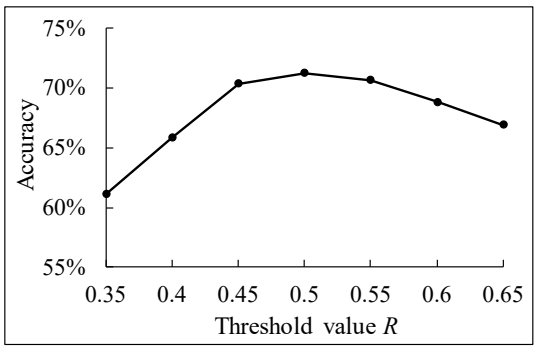

Fig. 5. *Accuracy of the lane selection against threshold R*

The comparison between the model estimation results and the surveyed data is shown in Table 5. There are four possible situations: the result of the proposed model is the same as the surveyed result (select the same lane), and the result of the proposed model is different from the surveyed result (select the different lane). In comparison, the model prediction for accepted gaps was based on a threshold of 0.5, which implies that any probability value below 0.5 was considered a selection of lane 1. The results show that 143 times out of 200 observations, the model concurred with the observed lane selection behaviour. The average accuracy of the lane selection estimation is 71.5%. The lane selection has a certain degree of randomness, especially when the utilities of choosing the two narrow lanes are comparable ($p(U)$ close to 0.5), e.g., the queue length of the two lanes are almost the same. According to Fig. 6, with the increase of the $|p(U)-0.5|$ value (the increase of the difference in utilities of choosing the two narrow lanes), the estimation accuracy increases significantly. It makes sense that the estimation accuracy is low when the calculated probability of choosing any of the two lanes is almost 50%. We further estimate the accumulate number of vehicles in the two narrow lanes, the accuracy is 95%. It means the traffic flow of the two narrow lanes can be well estimated although there is a kind of randomness when the utilities of choosing the two narrow lanes are comparable.

Table 5 Model validation of segment 2

Observed		Predicted Lane selection		Percentage
		Lane 1	Lane 2	Correct
Lane selection	Lane 1	67	31	68.4
	Lane 2	26	76	74.5
Overall Percentage				71.5

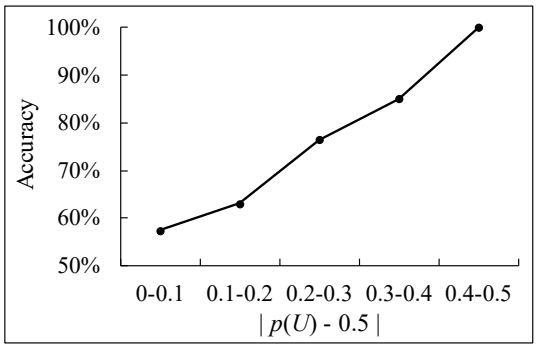

Fig. 6. *Accuracy of the lane selection against p(U)*

4.3. Segment 3

A sample of 999 vehicles was observed and used for model calibration and validation. There is not much difference with section 1 as the same procedural steps were followed. However, two more parameters need to be calibrated. The nonlinear regression was conducted using Levenberg-Marquardt estimation method. The results are shown in Table 6. The R-squared is 0.777.

Table 6 Parameter estimates of segment 3

Parameter	Estimate	Std. Error	95% Confidence Interval Lower Bound	Upper Bound
κ	0.320	0.011	0.297	0.342
λ	0.155	0.010	0.137	0.174
V_1	-1.743	0.445	-2.616	-.870
V_2	0.001	36.649	-71.940	71.942
C_1	0.040	0.004	0.031	0.048
C_2	-3.390	15.003	-29.455	29.448
C_3	0.026	0.013	0.001	0.051
C_4	0.013	0.003	0.008	0.018

The two-related-samples non-parametric test (Wilcoxon signed-rank method) was conducted to validate the accuracy of the model in segment 3. The results show that there is no significant difference between the estimated results from the model and the measured values, and thus it passes the validity test ($p > 0.05$) (Table 7).

Table 7 Model validation of segment 3

Items	N	Mean Rank	Sum of Ranks
Negative Ranks	95[a]	104.74	9950.00
Positive Ranks	104[b]	95.67	9950.00
Ties	0[c]		
Total	199		
Z	0.000		
Sig. (2-tailed)	1.000		

Note: a. Estimated < Measured; b. Estimated > Measured; c. Estimated = Measured

5. Simulation realization

The proposed model was accomplished in MATLAB (R2018a). The simulation process is described in Fig. 7, in which the time is discretized with a time step Δt. The vehicular trajectories of a numerical example are shown in Fig. 8. The parameters used in the numerical example are defined as follows. The discretized time step is 0.1 s. The start and end of the analysis area are between 0 m and 500 m. The lengths of the entering segment, transition section, special width lane segment, and exiting segment, are 200 m, 40 m, 120 m, and 140 m, respectively. The position of the stop line is 280 m. The signal cycle time is 60 s. The green time for through movement is from 0 s to 27 s in the cycle time. The total volume of vehicles is 600 veh/h. The heavy vehicle proportion is 10%. The maximum and minimum acceleration limitation are 5 m/s^2 and -8 m/s^2. The length of passenger cars and heavy vehicles are set to be 6 m and 12, respectively. The threshold value R for lane selection is 0.5. The parameters of the proposed model use the calibrated values in section 4.

One can find that the proposed model can reflect the operational phenomena of the SWAL, e.g., the normal car-following behaviour in the entering segment (segment 1), the lane selection behaviour in the transition segment (segment 2), the driving behaviour of passenger cars (driving alongside each other) and heavy vehicles (occupying two lanes) in the special width lane segment (segment 3), and the merging behaviour in the exiting segment (segment 4).

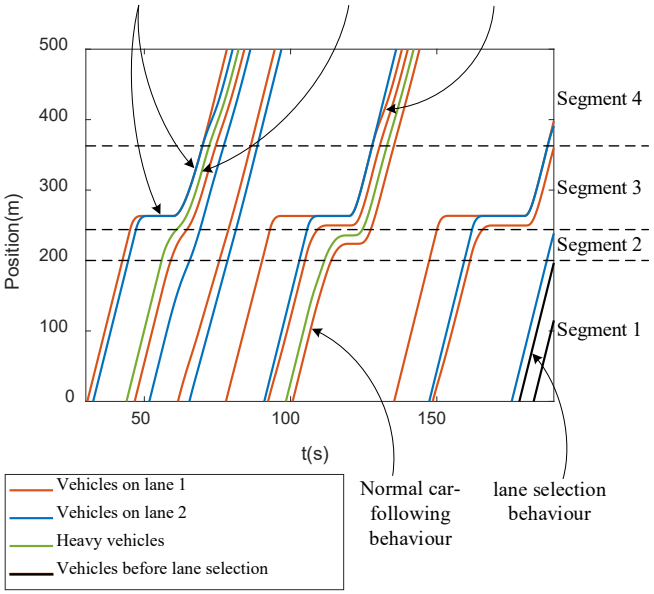

Fig. 8. *Vehicular trajectories of the simulation result*

6. Sensitivity analysis

Numerous numerical tests were conducted to investigate the impact of different geometric conditions, traffic conditions, and signal conditions on the effectiveness of the design. The other input parameters were kept the same as in section 5. The average vehicular delay is used as the indicator. The analysis duration is 1 hour for each run of the simulation. The results of 10 runs with different random seed are used for comparison to overcome the stochastic nature.

(1) Impact of the length of the SWAL

The length of the SWAL determines the number of queuing vehicles during the red time. It is set from 10 m to 60 m. The comparison result of the average vehicular delay is shown in Fig. 9.

Overall, with an increase in the length of the SWAL, more vehicles can be accommodated in the SWAL during the red phase. The effectiveness in reducing vehicular delay is very significant under high delay cases (over-saturated). It indicates that the setting of the SWAL can improve capacity. When the traffic condition is under-saturated (the length of the SWAL equals to 30 m in this case), the benefit of the SWAL in reducing delay becomes slight. It is in accordance with the changing tendency of delay with the degree of saturation in HCM [49]. However, with the further increase in the length of the SWAL, almost no benefit can be gain. It indicates that the SWAL cannot be too long because the passenger cars on the narrowed lanes cannot drive as efficiently as on the normal width lane.

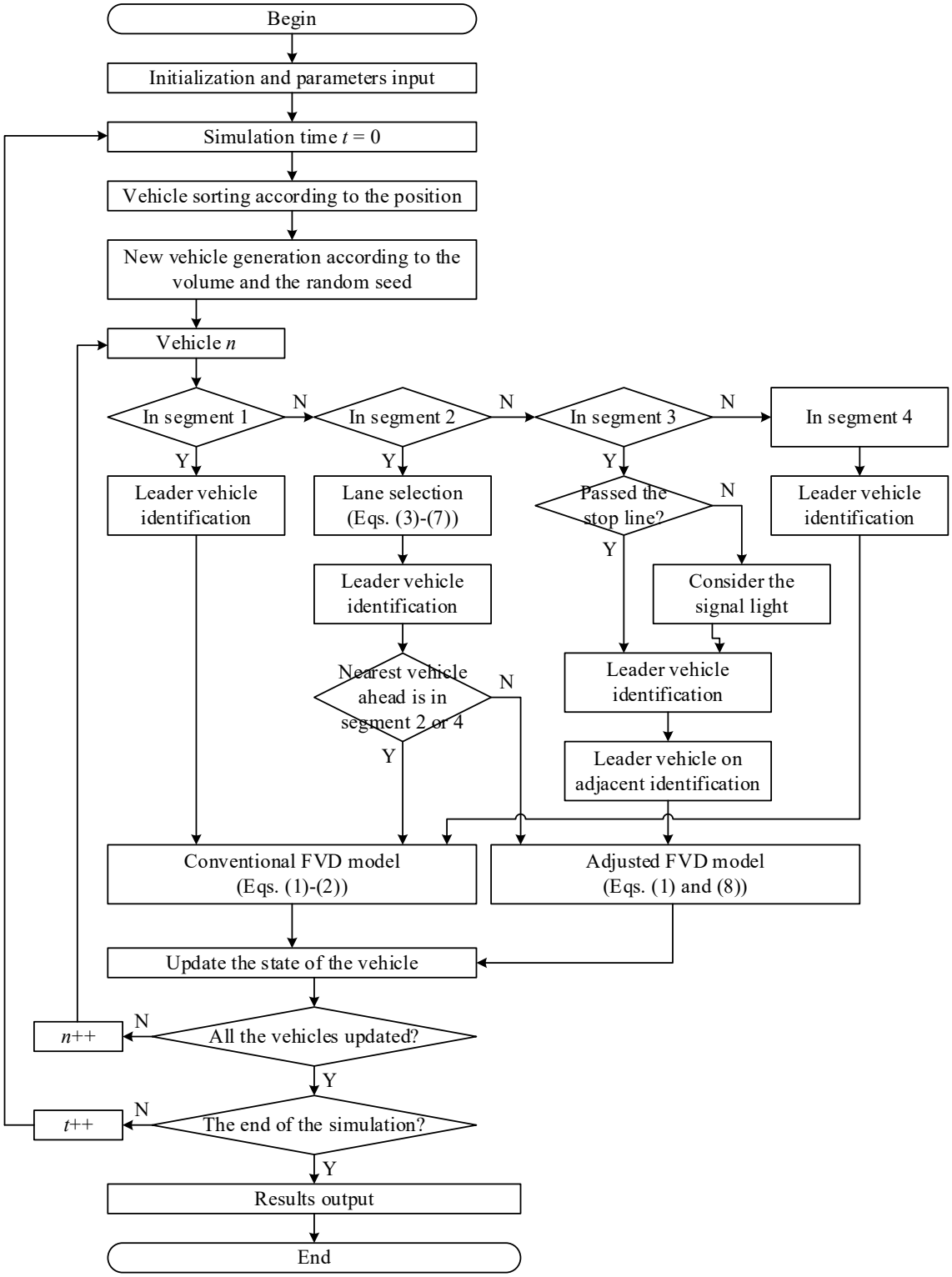

Fig. 7. *Simulation procedure of the proposed model*

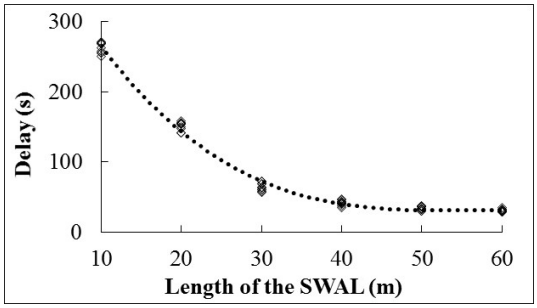

Fig. 9. *Impact of the length of the SWAL.*

(2) Impact of the volume and heavy vehicles

The SWAL design aims to improve the capacity of the intersection. However, the existence of the heavy vehicle may reduce the effectiveness because it should occupy the two lanes in the SWAL. Therefore, for traffic conditions, the total traffic volume and the percentage of heavy vehicles are the two key factors influencing the performance of the intersection with SWAL. In this experiment, the total traffic volume is set from 200 veh/h to 800 veh/h, and the percentage

of heavy vehicles is set from 0% to 30%. The comparison result is shown in Fig. 10.

The average vehicular delay increases with the increase of the volume and the percentage of heavy vehicles. The increase is smooth at first. Then, the delay rapidly increases when the volume is higher than 600 veh/h and the percentage of heavy vehicles is larger than 20%. The changing tendency is in accordance with the result of the previous study that the SWAL design is more suitable for the condition with a low percentage of heavy vehicles [15].

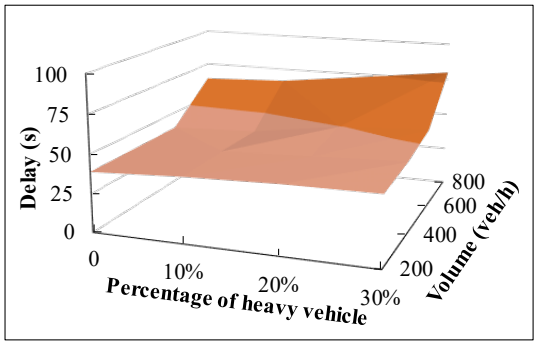

Fig. 10. *Impact of the traffic conditions.*

(3) Impact of the signal timing

Due to the limited length of the SWAL, the cycle length and green ratio become the key factors influencing the performance of the intersection with SWAL for signal conditions. In this experiment, the cycle length is set from 30 s to 120 s, and the green ratio is set from 0.3 to 0.6. The comparison result is shown in Fig. 11.

With the increase of the cycle length and the decrease of the green ratio, more vehicles need to wait during the red phase. Then, more room is needed for queuing. One can find the vehicular delay increases gently when the cycle length is short and the green ratio is high. Then, the delay rapidly increases when the cycle length is longer than 90 s and the green ratio is lower than 0.4. It is due to the fact that more vehicles have to wait in front of the stop line in these scenarios. The SWAL is not long enough to accommodate the queuing vehicles. It indicates that for the design of the intersection with SWAL, the layout design and the signal control should be integrated. The limitation of the length of the SWAL should be fully considered in signal timing.

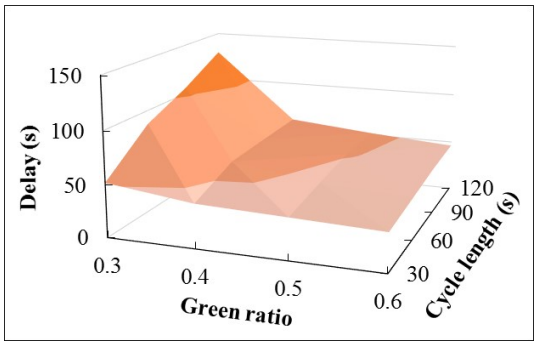

Fig. 11. *Impact of the signal conditions.*

7. Conclusion

A microscopic traffic flow model was proposed for describing the operation of vehicles at signalized intersections with SWAL. The proposed model was realized in a time-discretized simulation. The sensitivity analysis of geometric, traffic, and signal factors were conducted. From the analysis, the following conclusions can be drawn.

(1) The proposed model and the corresponding simulation process can describe the operation of driving on the SWAL by combining the car-following and lane selection behaviours.

(2) All the parameters are also calibrated using the field data. For the car-following behaviour, it shows that the passenger cars on the narrowed lanes cannot be driven as efficient as on the normal width lane. For the lane selection behaviour, it mainly depends on the distance between the two nearest vehicles in front on the two narrow lanes.

(3) The analysis of the sensitivity shows that the effectiveness of the SWAL mainly depends on whether it is long enough to accommodate the queuing vehicles, which is a combined result of the layout design and the signal timing.

Please note that the driving behaviour parameters recommended in the paper are based on the field data collected in Germany. The driver behaviour may be affected by many factors, including the time of day, surrounding traffic environment, and the site. Moreover, for unconventional design, the driver behaviour may also change with the time that it has been set for the study, which can be the direction of our further study.

8. Acknowledgments

This work was supported in part by the National Natural Science Foundation of China under Grant 71971140. Thank Dr. Bastian Chlond from Karlsruhe Institute of Technology for providing us the information on the survey site. Thank Dr. Zi Wang from Karlsruhe Institute of Technology for helping us during the survey.

9. References

[1] Hummer, J.E., 'Unconventional Left-Turn Alternatives for Urban and Suburban Arterials - Part One', *ITE journal*, 1998, 68, (9), pp. 26-29.

[2] Liu, P., Lu, J.J., and Chen, H., 'Safety Effects of the Separation Distances between Driveway Exits and Downstream U-Turn Locations', *Accident Analysis and Prevention*, 2008, 40, (2), pp. 760-767.

[3] Holzem, A.M., Hummer, J.E., Cunningham, C.M., O'Brien, S.W., Schroeder, B.J., and Salamati, K., 'Pedestrian and Bicyclist Accommodations and Crossings on Superstreets', *Transportation Research Record*, 2015, 2486, (1), pp. 37-44.

[4] Moon, J.P., Kim, Y.R., Kim, D.G., and Lee, S.K., 'The Potential to Implement a Superstreet as an Unconventional Arterial Intersection Design in Korea', *KSCE Journal of Civil Engineering*, 2011, 15, (6), pp. 1109-1114.

[5] Liu, Y. and Luo, Z.K., 'A Bi-Level Model for Planning Signalized and Uninterrupted Flow Intersections in an Evacuation Network', *Computer-Aided Civil And Infrastructure Engineering*, 2012, 27, (10), pp. 731-747.

[6] Jagannathan, R. and Bared, J.G., 'Design and Operational Performance of Crossover Displaced Left-Turn Intersections', *Transportation Research Record*, 2004, 1881, (1), pp. 1-10.

[7] Suh, W. and Hunter, M.P., 'Signal Design for Displaced Left-Turn Intersection Using Monte Carlo Method', *KSCE Journal of Civil Engineering*, 2014, 18, (4), pp. 1140-1149.

[8] Zhao, J., Ma, W., Zhang, H.M., and Yang, X., 'Increasing the Capacity of Signalized Intersections with Dynamic Use of Exit Lanes for Left-Turn Traffic', *Transportation Research Record*, 2013, 2355, (1), pp. 49-59.
[9] Wu, J., Liu, P., Tian, Z.Z., and Xu, C., 'Operational Analysis of the Contraflow Left-Turn Lane Design at Signalized Intersections in China', *Transportation Research Part C: Emerging Technologies*, 2016, 69, pp. 228-241.
[10] Chen, Q., Yi, J.X., and Wu, Y.L., 'Cellular Automaton Simulation of Vehicles in the Contraflow Left-Turn Lane at Signalised Intersections', *Iet Intelligent Transport Systems*, 2019, 13, (7), pp. 1164-1172.
[11] Xuan, Y., Daganzo, C.F., and Cassidy, M.J., 'Increasing the Capacity of Signalized Intersections with Separate Left Turn Phases', *Transportation Research Part B: Methodological*, 2011, 45, (5), pp. 769-781.
[12] Ma, W., Xie, H., Liu, Y., Head, L., and Luo, Z., 'Coordinated Optimization of Signal Timings for Intersection Approach with Presignals', *Transportation Research Record*, 2013, 2355, (1), pp. 93-104.
[13] Yan, C., Jiang, H., and Xie, S., 'Capacity Optimization of an Isolated Intersection under the Phase Swap Sorting Strategy', *Transportation Research Part B: Methodological*, 2014, 60, pp. 85-106.
[14] Zhao, J., Li, P., Zheng, Z., and Han, Y., 'Analysis of Saturation Flow Rate at Tandem Intersections Using Field Data', *Iet Intelligent Transport Systems*, 2018, 12, (5), pp. 394-403.
[15] Zhao, J., Liu, Y., and Wang, T., 'Increasing Signalized Intersection Capacity with Unconventional Use of Special Width Approach Lanes', *Computer-Aided Civil And Infrastructure Engineering*, 2016, 31, (10), pp. 794-810.
[16] Thompson, I., Dam, T., and Nielsen, J.B., *European Landscape Architecture: Best Practice in Detailing*, (Routledge, 2007)
[17] Parkin, J. and Meyers, C., 'The Effect of Cycle Lanes on the Proximity between Motor Traffic and Cycle Traffic', *Accident Analysis & Prevention*, 2010, 42, (1), pp. 159-165.
[18] Bauer, K.M., Harwood, D.W., Hughes, W.E., and Richard, K.R., 'Safety Effects of Narrow Lanes and Shoulder-Use Lanes to Increase Capacity of Urban Freeways', *Transportation Research Record*, 2004, 1897, (1), pp. 71-80.
[19] Hamilton-Baillie, B., 'Towards Shared Space', *Urban Design International*, 2008, 13, (2), pp. 130-138.
[20] Anvari, B., Daamen, W., Knoop, V.L., Hoogendoorn, S.P., and Bell, M.G., Shared Space Modeling Based on Social Forces and Distance Potential Field', in Ulrich Weidmann, U.K., Michael Schreckenberg (ed.), *Pedestrian and Evacuation Dynamics 2012*, (Springer, 2014)
[21] Yuan, Y., Goñi-Ros, B., van Oijen, T.P., Daamen, W., and Hoogendoorn, S.P., Social Force Model Describing Pedestrian and Cyclist Behaviour in Shared Spaces', *International Conference on Traffic and Granular Flow*, (Springer, 2017)
[22] Anvari, B., Bell, M.G., Sivakumar, A., and Ochieng, W.Y., 'Modelling Shared Space Users Via Rule-Based Social Force Model', *Transportation Research Part C: Emerging Technologies*, 2015, 51, pp. 83-103.
[23] AASHTO, *A Policy on Geometric Design of Highways and Streets*, (American Association of State Highway and Transportation Officials (AASHTO), 2011, 6th Edition edn)
[24] Fuller, R., 'The Task-Capability Interface Model of the Driving Process', *Recherche-Transports-Sécurité*, 2000, 66, pp. 47-57.
[25] Zhao, J. and Zhou, X., 'Improving the Operational Efficiency of Buses with Dynamic Use of Exclusive Bus Lane at Isolated Intersections', *IEEE Transactions on Intelligent Transportation Systems*, 2019, 20, (2), pp. 642-653.
[26] Gupta, A.K. and Katiyar, V.K., 'A New Anisotropic Continuum Model for Traffic Flow', *Physica A: Statistical Mechanics and its Applications*, 2006, 368, (2), pp. 551-559.
[27] Yu, S.W., Huang, M.X., Ren, J., and Shi, Z.K., 'An Improved Car-Following Model Considering Velocity Fluctuation of the Immediately Ahead Car', *Physica A: Statistical Mechanics and its Applications*, 2016, 449, pp. 1-17.
[28] Zhu, W.X. and Zhang, H.M., 'Analysis of Mixed Traffic Flow with Human-Driving and Autonomous Cars Based on Car-Following Model', *Physica A: Statistical Mechanics and its Applications*, 2018, 496, pp. 274-285.
[29] Li, L., Jiang, R., and Jia, B., *Modern Traffic Flow Theory and Application*, (Tsinghua University Press, 2011)
[30] Helbing, D. and Tilch, B., 'Generalized Force Model of Traffic Dynamics', *Physical Review E*, 1998, 58, (1), pp. 133-138.
[31] Nagatani, T., 'Stabilization and Enhancement of Traffic Flow by the Next-Nearest-Neighbor Interaction', *Physical Review E*, 1999, 60, (6), pp. 6395-6401.
[32] Jiang, R., Wu, Q., and Zhu, Z., 'Full Velocity Difference Model for a Car-Following Theory', *Physical Review E*, 2001, 64, (1), p. 017101.
[33] Zhao, X. and Gao, Z., 'A New Car-Following Model: Full Velocity and Acceleration Difference Model', *The European Physical Journal B-Condensed Matter and Complex Systems*, 2005, 47, (1), pp. 145-150.
[34] Zhao, J., Knoop, V.L., and Wang, M., 'Two-Dimensional Vehicular Movement Modelling at Intersections Based on Optimal Control', *Transportation Research Part B: Methodological*, 2020, 138, pp. 1-22.
[35] Jia, D., Ngoduy, D., and Vu, H.L., 'A Multiclass Microscopic Model for Heterogeneous Platoon with Vehicle-to-Vehicle Communication', *Transportmetrica B-Transport Dynamics*, 2019, 7, (1), pp. 448-472.
[36] Zhang, X.H., Sun, J., Qi, X., and Sun, J., 'Simultaneous Modeling of Car-Following and Lane-Changing Behaviors Using Deep Learning', *Transportation Research Part C-Emerging Technologies*, 2019, 104, pp. 287-304.
[37] Zhang, J., Tang, T.Q., and Wang, T., 'Some Features of Car-Following Behaviour in the Vicinity of Signalised Intersection and How to Model Them', *Iet Intelligent Transport Systems*, 2019, 13, (11), pp. 1686-1693.
[38] Guo, L., Zhao, X., Yu, S., Li, X., and Shi, Z., 'An Improved Car-Following Model with Multiple Preceding Cars' Velocity Fluctuation Feedback', *Physica A: Statistical Mechanics and its Applications*, 2017, 471, pp. 436-444.
[39] Zhao, J. and Liu, Y., 'Safety Evaluation of Intersections with Dynamic Use of Exit-Lanes for Left-Turn Using Field Data', *Accident Analysis and Prevention*, 2017, 102, pp. 31-40.
[40] Zhao, J., Malenje, J.O., Tang, Y., and Han, Y., 'Gap Acceptance Probability Model for Pedestrians at Unsignalized Mid-Block Crosswalks Based on Logistic

Regression', *Accident Analysis & Prevention*, 2019, 129, pp. 76-83.
[41] Tang, T., Wu, Y., Caccetta, L., and Huang, H., 'A New Car-Following Model with Consideration of Roadside Memorial', *Physics Letters A*, 2011, 375, (44), pp. 3845-3850.
[42] Habel, L. and Schreckenberg, M., Asymmetric Lane Change Rules for a Microscopic Highway Traffic Model', in Was, J., Sirakoulis, G.C., and Bandini, S. (eds.), *Cellular Automata: 11th International Conference on Cellular Automata for Research and Industry*, (2014)
[43] Naito, Y. and Nagatani, T., 'Safety–Collision Transition Induced by Lane Changing in Traffic Flow', *Physics Letters A*, 2011, 375, (10), pp. 1319-1322.
[44] Choudhury, C.F. and Ben-Akiva, M.E., 'Lane Selection Model for Urban Intersections', *Transportation Research Record*, 2008, 2088, (1), pp. 167-176.
[45] Liu, P., Xu, C., Wang, W., and Wan, J., 'Identifying Factors Affecting Drivers' Selection of Unconventional Outside Left-Turn Lanes at Signallised Intersections', *Iet Intelligent Transport Systems*, 2013, 7, (4), pp. 396-403.
[46] Aghabayk, K., Sarvi, M., and Young, W., 'Attribute Selection for Modelling Driver's Car-Following Behaviour in Heterogeneous Congested Traffic Conditions', *Transportmetrica A: Transport Science*, 2014, 10, (5), pp. 457-468.
[47] Zheng, L., Jin, P.J., Huang, H., Gao, M., and Ran, B., 'A Vehicle Type-Dependent Visual Imaging Model for Analysing the Heterogeneous Car-Following Dynamics', *Transportmetrica B: Transport Dynamics*, 2016, 4, (1), pp. 68-85.
[48] Nagahama, A., Yanagisawa, D., and Nishinari, K., 'Car-Following Characteristics of Various Vehicle Types in Respective Driving Phases', *Transportmetrica B: Transport Dynamics*, 2020, 8, (1), pp. 22-48.
[49] TRB, *Highway Capacity Manual 2010*, (Transportation Research Board, 2010)